How ocean color can steer Pacific tropical cyclones

Anand Gnanadesikan[1]
Kerry Emanuel[2]
Gabriel A. Vecchi[1]
Whit G. Anderson[1]
Robert Hallberg[1]

1: NOAA Geophysical Fluid Dynamics Laboratory, Princeton NJ
2: Dept. of Earth, Atmosphere and Planetary Sciences, MIT, Cambridge, MA

Submitted to Geophysical Research Letters

Abstract

Because ocean color alters the absorption of sunlight, it can produce changes in sea surface temperatures with further impacts on atmospheric circulation. We demonstrate these changes can project onto fields previously recognized to alter the distribution of tropical cyclones. If the North Pacific subtropical gyre contained no absorbing and scattering materials, the result would be to reduce tropical cyclone activity in the Northwest Pacific by 2/3. We also demonstrate that much smaller changes in the formulation of solar absorption can have significant impacts on the spatiotemporal distribution of tropical cyclones with greater penetration moving tropical cyclones closer to the equator. Changes in ocean biogeochemical cycles may thus have implications for tropical cyclone activity.

1. Introduction

Scattering and absorbing materials in seawater affect the degree to which sunlight penetrates into the ocean interior. In very clear waters, less sunlight is absorbed close to the air-sea interface, reducing sea surface temperatures (SSTs) and warming subsurface waters (Morel, 1988; Lewis et al., 1990) which may then be brought to the surface in upwelling regions on decadal time scales. The resulting patterns of change in SST can feed back onto changes in atmospheric circulation (Shell et al., 2001). Recent work with global, fully coupled climate models has shown that off-equatorial impact of removing ocean color may be larger than previously realized (Lengaigne et al., 2007; Anderson et al., 2007; Gnanadesikan and Anderson, 2009), reducing SSTs by up to 1.8C. In this work we examine the implications of these changes for the formation of tropical cyclones (TCs) in the Pacific basin.

The Northwest Pacific is the most active basin for TCs, experiencing an average of 131 “TC days” each year; vs. 61 for the Atlantic and 58 for the Northeast Pacific, and accounting for 55% of reported hurricane-force winds over the past 25 years (Maue et al., 2008). Between 1990 and 1998, damage from cyclones in the Asia Pacific region averaged over $3B with 740 deaths per year (Saunders et al., 2000). As shown in Figure 1a, many 5° bins in of this region see winds over 17m/s for more than four days out of every year and experience multiple genesis events each decade. Variation in both the occurrence and paths of TCs have been tied to the El Nino Southern Oscillation (Chan and Liu, 2004). Models are able to recover these interannual variations (Zhao et al., in press) suggesting that they are strongly controlled by large-scale environmental

conditions. In this paper we use a global coupled climate model to assess the changes in the upper ocean thermal structure and mean atmospheric circulation produced by a changing the ocean's profile of solar heating, and then use two techniques to examine the potential of these impacts on TCs. We demonstrate that the presence of ocean color has a first-order impact on the spatiotemporal distribution of TCs so that even small details in the representation of upper ocean absorption can have significant impacts on predictions of TC activity.

2. Methods

a.) Coupled climate model

The atmosphere, land, and sea ice modules for this model are those used in the Geophysical Fluid Dynamics Laboratory CM2.1 model (Delworth et al., 2006) which produced one of the most realistic simulations of modern climate submitted to the Intergovernmental Panel on Climate Change Fourth Assessment report (Reichler and Kim, 2008). The ocean model used for the first set of simulations is the Hallberg Isopycnal Model code, an isopycnal layer-coordinate ocean model with realistic equation of state, Richardson number-dependent mixing, and a four-layer representation of the mixed layer (Hallberg and Gnanadesikan, 2006). An updated version of this code (the Generalized Ocean Layer Dynamics model, Hallberg and Adcoft, 2009) is used for a second set of runs. Use of an isopycnal model minimizes the unrealistic impacts of numerical discretization on vertical mixing (Griffies et al., 2000) and allowing temperature perturbations to persist longer than in traditional level-coordinate models.

The optical scheme is based on the data of Morel (1988) as reanalyzed by Manizza et al. (2005). This formulation breaks the incoming shortwave radiation at the surface into three bands, 58% near-IR, 21% red-yellow, and 21% blue-green each with a chlorophyll-dependent attenuation scale. In our first set of runs, the surface layer was 10m deep, so that it made little sense to resolve the near-IR and red-yellow bands which have e-folding depths less than 5m. Thus our scheme was further simplified to only allow penetration of the blue-green portions. Chlorophyll concentrations for our control (Green) run were taken from the SeaWiFS satellite (Yoder and Kennelly, 2003; Sweeney et al., 2005). Perturbation runs were made where a.) chlorophyll was set to zero in the Pacific within 30 degrees of the equator when concentrations dropped below 0.2 mg/m^3 (perturbation run BLPGyre), shown by the hatching in Fig.2a.) b.) reduced by 50% globally (perturbation run Half).

Since such large changes are somewhat extreme, we also wanted to investigate the potential impact of smaller changes in the formulation of shortwave absorption- the sorts of choices that climate modelers might easily make without thinking carefully about the implications for TC activity. In a second set of runs the minimum mixed layer depth was set to 2m and two more runs were performed, one using one band as in the previous simulation and a second run with the full three-band parameterization.

b.) Impact on TC formation

We estimate the impact of SST on TC activity using two techniques. The first is an empirically-derived Genesis Potential Index (GPI) relating environmental conditions to the number of TCs found in different regions. Following Camargo et al. (2007)

$$GPI = (PI/70)^3 \times (1 + 0.1 * |U_{200} - U_{850}|)^{-2} \times (RH_{700}/50)^3 \times (Vort_{850} \times 10^5)^{3/2} \quad (1)$$

In this formula PI is the potential intensity. U_{200}-U_{850} is the shear of the zonal wind between the 200 mb and 850 mb in m/s, RH_{700} is the relative humidity at 700mb in percent and $Vort_{850}$ is the absolute vorticity (curl of the vector horizontal wind + Coriolis parameter) at 850mb in s^{-1}.

PI is based on a line of theoretical papers linking the dynamics and thermodynamics of a TCs. Serving as a measure of the thermodynamic disequilibrium between the ocean and atmosphere, it represents the peak intensity the storm can attain under ideal conditions. GPI builds upon the PI, accounting for the effects of vorticity in creating conditions that are more favorable for convective organization, shear in preventing such organization, and low relative humidity in the middle of the atmosphere in inhibiting storm formation and maintenance. GPI has been used to evaluate changes in cyclogenesis associated with ENSO (Camargo et al., 2007), intraseasonal oscillations (Camargo et al., 2009) and climate change (Vecchi and Soden, 2007). The GPI in our control run (Fig. 1b) captures the magnitude of cyclogenesis, with a band in which 8-9 storms are generated per decade in a given 5° bin. The location of this band, however is offset equatorward by 5-10°, indicating biases in the modeled atmospheric circulation and/or the GPI method.

The second technique is the statistical-dynamical downscaling of Emanuel (2006). This technique involves randomly seeding the tropics with weak, warm-core vortices that

are then advected by the large-scale steering flow. The steering flow consists of synthetic time series of winds at two levels whose monthly mean, variances, and covariances are those of the coupled model. The result is to produce an ensemble of paths which track through spatially-varying environmental conditions. The resulting paths and environmental conditions are used to drive a simple radially symmetric, coupled atmosphere-ocean model that then predicts the intensity and size of the cyclone that develops. It should be noted that the vast majority of vortices do not develop into hurricane-strength storms. This approach neglects the possibility that changes in the climatology of the triggering disturbances (rather than the development of these disturbances) could be responsible for variability in tropical cyclogenesis. The predicted distribution of cyclones (Fig. 1c) from our control run reproduces the pattern of TC frequency with a correlation coefficient of 0.89 and TC genesis with a correlation coefficient of 0.72.

3. Results

a.) Impact of clear subtropical gyres

As seen in Fig. 2, increasing the penetration depth of solar radiation from ~20m to ~40m in the low chlorophyll subtropical gyres (shown by the hatching in Fig. 2a) leads to changes in quantities that affect the GPI. SSTs in the gyres drop and subsurface waters warm- subsequently upwelling along the Equator on time scales of five to ten years. This pattern of SST change (Fig. 2a) leads to a strengthening of the atmospheric Hadley circulation, with flow from the cold to the warm anomaly (vectors, Fig. 2a). The resulting

upward motion and precipitation along the Equator increases outflow aloft (Fig. 2b). As the outflow moves away from the equator it is turned eastward by the Coriolis force, producing higher westerly winds. Intensification of the sinking branch of the Hadley circulation (Fig. 2b) transports more dry air into the lower troposphere, causing both a reduction in relative humidity (Fig. 2c) and, by compressing the air column, decreasing its cyclonic vorticity.(Fig. 2d).

Comparing the GPI in the BluePGyre and Control runs shows drops over the subtropical zones and increases in the near-equatorial region (Fig. 3a). Using the GPI we can evaluate both the total change associated with the differences illustrated in Fig. 2 by replacing all the fields in (1) as well as identifying which fields are most important by replacing each one sequentially. In the off-equatorial region (Fig 3b), a 70% total drop in genesis potential involves contributions from all four factors. Wind shear appears to be the largest of these, followed by potential intensity and relative humidity, with vorticity playing a small role.

The statistical-dynamical downscaling technique shows a similar shift in TC frequency and genesis (Fig. 3c) The tracks in the run with clear gyres are much more focused near the equator, with more storms tracking into the South China Sea, but virtually no tracks moving into the East China Sea and many fewer landfalls in Japan and South China. The changes in genesis are roughly the same magnitude as those predicted by the GPI. Zonally averaged changes in TC frequency (Fig. 3d), show an increase in the equatorial zones, and a decrease approaching 60% in the higher latitudes. This decrease is more pronounced for typhoons (max winds > 33 m/s) than for all TCs; implying that

not only the location but the intensity of TCs could be affected by changes in ocean color distributions.

b.) Impact of shortwave absorption formulation

The direction of the change from one-band to three-band (representing a change in model formulation) is thus similar in direction to the change between our Control and BluePGyre simulations discussed above- allowing more penetration of sunlight. The resulting SST changes (Fig. 4a) are much smaller than those associated with clearing the subtropical gyre but still amount to a warming in the Pacific of 0.4ºC in the cold tongue and a cooling of the same magnitude off of Mexico. The warming over the cold tongue produces an upper-level outflow (vectors in Fig. 4a) that overlies the cold patch off Mexico. Local changes in GPI (Fig. 4b) are still potentially significant, with a maximum decrease of 2.2. Analysis of the driving mechanisms shows that as with the West Pacific, shear response plays the most important role.

Downscaling runs based on the more realistic three-band run (Figure 4c) show a pattern of TC activity that reproduces the observed triangular pattern of occurrence, with a high near 20N, 120W and a zone of high TC activity stretching to the west along 20N (the correlation coefficient is 0.72). Relative to the case where only one band is used, the distribution of cyclones is realistically shifted southward (Fig. 4d) with a 24% decrease in TC activity off of Baja California (25N-35N, 140W-110W) and a 17% increase off of Hawaii (10N-20N, 175W-160W). Cyclogenesis changes (contours in Fig. 4d) are roughly consistent with the GPI changes, with reductions of up to 1.5 genesis events per

5º box per decade to the north and increases in cyclogenesis of 0.2-0.4 genesis events per 5º box per decade to the south. The results are even more striking when only hurricanes are considered, with a 25% increase off Hawaii and a 39% decrease off Baja California.

4. Discussion and conclusions

We have shown that the presence of light-absorbing material substantially shapes the paths of Pacific TCs, allowing them to propagate to higher latitudes. How much could this change over time? While removing all excess absorbing materials is obviously extreme, there is evidence (Karl et al.,2001) that during the 1960s chlorophyll levels in Pacific subtropical gyres were 50% lower than at present- although it is unclear how much of the change is due to differences in measurement techniques. When chlorophyll is reduced by a factor by 50% in our coupled model the resulting atmosphere produces a GPI about 35% lower in the subtropical NW Pacific, about half the drop seen in Fig. 3a. This change is consistent with lower typhoon activity in the 1960s, suggesting that some part of the increase since this time could be due to changes in nutrient supply or iron deposition. Our results more attention be paid to the mechanisms modulating the injection of heat into the upper thermocline of tropical regions.

References

Anderson, W.G., A. Gnanadesikan, A., R.W. Hallberg, J.P. Dunne, and B.L. Samuels, (2007) Impact of ocean color on the maintenance of the Pacific Cold Tongue, *Geophys. Res. Lett.*, 34, L11609, doi:10.1029/2007GL030100.

223 Anderson,W.G, A. Gnanadesikan and A.T. Wittenberg, (2009) Regional impacts of
224 ocean color on tropical Pacific variability, *Ocean Science*,5,313-327.
225 Camargo, S., K. Emanuel, and A.H. Sobel, (2007) Use of a genesis potential index to
226 diagnose ENSO effects on tropical cyclone genesis, *J. Climate*, 20, 4819—4833.
227 Camargo, S., M.C. Wheeler and A.H. Sobel (2009) Diagnosis of the MJO modulation of
228 tropical cyclogenesis using an empirical index, *J. Atmos. Sci.*, 3061-3074, (2009)
229 Chan J.C.L. and K.S. Liu (2004) . Global warming in North Pacific typhoon activity from
230 an observational perspective, *J. Climate*, 17, 4590-4602.
231 Delworth,T. *et al.* , (2006) GFDL's CM2 global coupled climate models- Part 1:
232 Formulation and simulation characteristics, *J. Climate*, 19, 643-674.
233 Emanuel, K., (2006) Climate and tropical cyclone activity: A model downscaling
234 approach, *J. Climate*, 19,4797-4802.
235 Gnanadesikan, A., and W.G. Anderson, (2009) Ocean water clarity and the ocean general
236 circulation in a coupled climate model, *J. Phys. Oceanogr.*, 39(2), 314-332.
237 Griffies, S.M., R.C. Pacanowski and R.W. Hallberg (2000) Spurious diapycnal mixing
238 associated with advection in a z-coordinate model, *Mon. Weather Rev*., 128, 538-
239 564.
240 Hallberg, R and A. Adcroft. (2009) Reconciling estimates of the free surface height in
241 Lagrangian vertical coordinate ocean models with mode-split time stepping.
242 *Ocean Modelling*, 29(1), 15-26, doi:10.1016/j.ocemod.2009.02.008.
243 Hallberg, R. and A. Gnanadesikan, (2006) The role of eddies in determining the structure
244 and response of the wind-driven Southern Hemisphere overturning: Results from

the Modeling Eddies in the Southern Ocean (MESO) project, *J. Phys. Oceanogr.*, *36*, 2232-2252.

Karl, D.M., R.R., Bidigare, and R.M. Letelier, (2001) Long-term changes in phytoplankton community structure and productivity in the North Pacific Subtropical Gyre- The domain shift hypothesis, *Deep Sea Res. II*, 48, 1449-1470.

Lengaigne, M., et al. (2007): Influence of the oceanic biology on the tropical Pacific climate in a coupled general circulation model, *Clim. Dyn., 28*, 503-516

Lewis, M. R., M. E. Carr, G. C. Feldman, W. Esaias, and C. McClain, (1990) Influence of penetrating solar radiation on the heat budget of the equatorial Pacific Ocean, *Nature*, *347*, 543– 545.

Manizza, M., C. Le Quere, A.J. Watson, E.T. Buitenhuis (2005) Bio-optical feedbacks among phytoplankton, upper ocean physics and sea ice in a global model, *Geophys. Res. Lett.*, 32, L05603, doi: 10.1029/20004GL020778.

Morel, A., (1988) Optical modeling of the upper ocean in relation to its biogenous matter content (case-I waters), J. Geophys. Res., 93, 10,749–10,768.

Maue, R.N., (2008) Northern Hemisphere tropical cyclone activity, *Geophys. Res. Lett.*, 36, L05805, doi:10.1029/2008GL035946.

Nakamoto, S., S. P. Kumar, J. M. Oberhuber, J. Ishizaka, K. Muneyama, and R. Frouin, (2001) Response of the equatorial Pacific to chlorophyll pigment in a mixed layer isopycnal ocean general circulation model, *Geophys. Res. Lett.*, 28, 2021– 2024.

Reichler, T. and J. Kim, (2008) How well do coupled climate models simulate today's climate, *Bull. Amer. Met. Soc.* 89, 303-311.

Shell, K. M., S. Nakamoto, R.C. Frouin and R.C. Somerville, (2003), Atmospheric response to solar radiation absorbed by phytoplankton, *J. Geophys. Res*., 108(D15), 4445, doi:10.1029/2003JD003440.

Saunders, M.A., R.E. Chandler, C.J. Merchant, and F.P. Roberts, (2000) Atlantic Hurricanes and NW Pacific typhoons: ENSO spatial impacts on occurrence and landfall, *Geophys. Res. Lett.*, 27, 1147-1150.

Sweeney, C., A. Gnanadesikan, S.M. Griffies, M.J. Harrison, A. Rosati, and B.L. Samuels, (2005) Impacts of shortwave penetration depth on large-scale ocean-circulation and heat transport, *J. Phys. Oceanogr.*, 35(6), 1103-1119.

Vecchi, G.A. and B.J. Soden (2007) Increased Atlantic wind shear in projections of global warming, *Geophys. Res. Lett*, 34, L08702, doi:10.1029/2006GL028905.

Yoder, J. A and M.A. Kennelly, M.A. (2003) Seasonal and ENSO variability in global ocean phytoplankton chlorophyll derived from 4 years of SeaWiFS measurements. *Global Biochem. Cycles*, 17 (4), 1112, doi:10.1029/2002GB001942.

Zhao, M.., Held, I, Lin S.-J. & Vecchi, G.A., Simulations of global hurricane climatology, interannual variability and response to global warming using a 50km resolution GCM, *J. Climate*, in press.

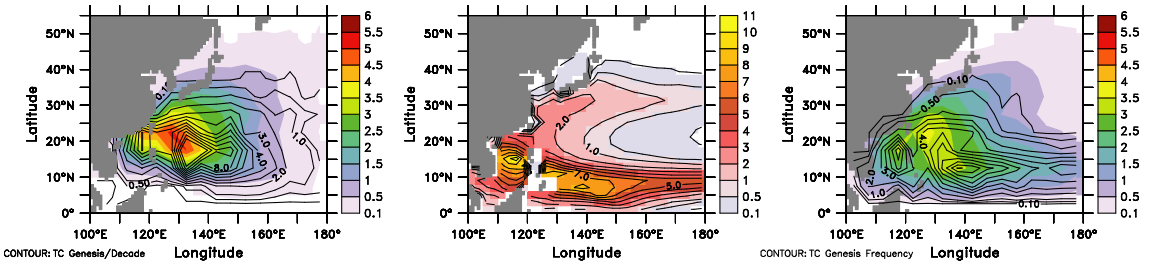

Figure 1: Cyclogenesis in the western North Pacific. (a) Observed TC days/year (one TC day means an entire day with a tropical storm within a 5 degree bin) from 1945-2008 and genesis within a five degree-bin/decade. Dataset compiled from NOAA Tropical Prediction Center for the North Atlantic and Eastern North Pacific and the Navy Joint Typhoon Warning Center for the rest of the globe. Available at ftp://texmex.mit.edu/pub/emanuel/HURR/tracks/). (b) Genesis Potential Index from control run. (c) TC frequency (days/yr/5 degree bin colors), and genesis frequency (storms/decade contours/5 degree bin) using the statistical-dynamical downscaling with environmental conditions given by control run.

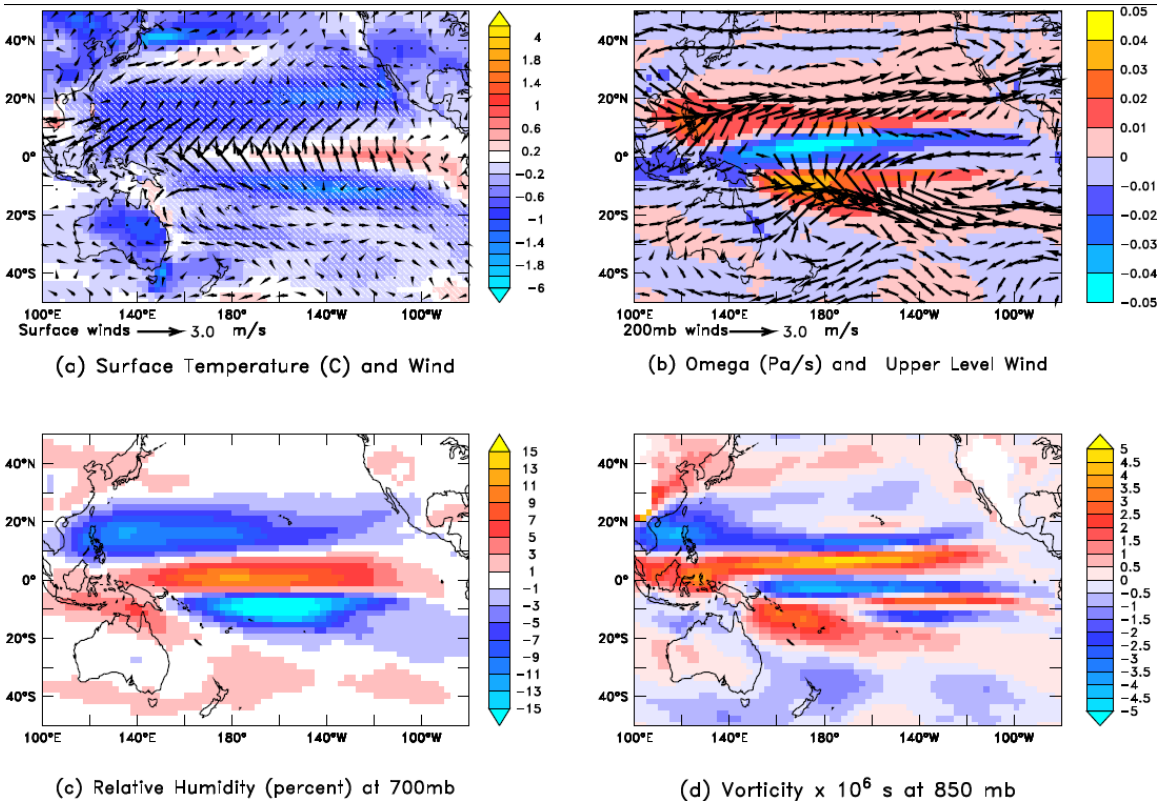

Figure 2: Changes in environmental conditions brought about by removing color-dependent absorption from low-chlorophyll regions in the subtropical gyres (shown by hatching in (a)) in a coupled climate model. All fields are annual averages from years 41-120. Since changes in these fields tend to be more extreme in the summer season, the impact on TC formation will in general be more pronounced than would be inferred from these plots. (a) Changes in surface temperature in degrees (colors) and 2m winds (vectors). (b) Changes in vertical velocity at 500m in pressure units of Pa/s (colors) and upper level winds at 200mb (vectors). (c) Changes in relative humidity at 700mb. (d) Changes in vorticity (curl of the horizontal velocity) at 850mb. In northern hemisphere, positive values are associated with lower pressures, while in the southern hemisphere the opposite is true.

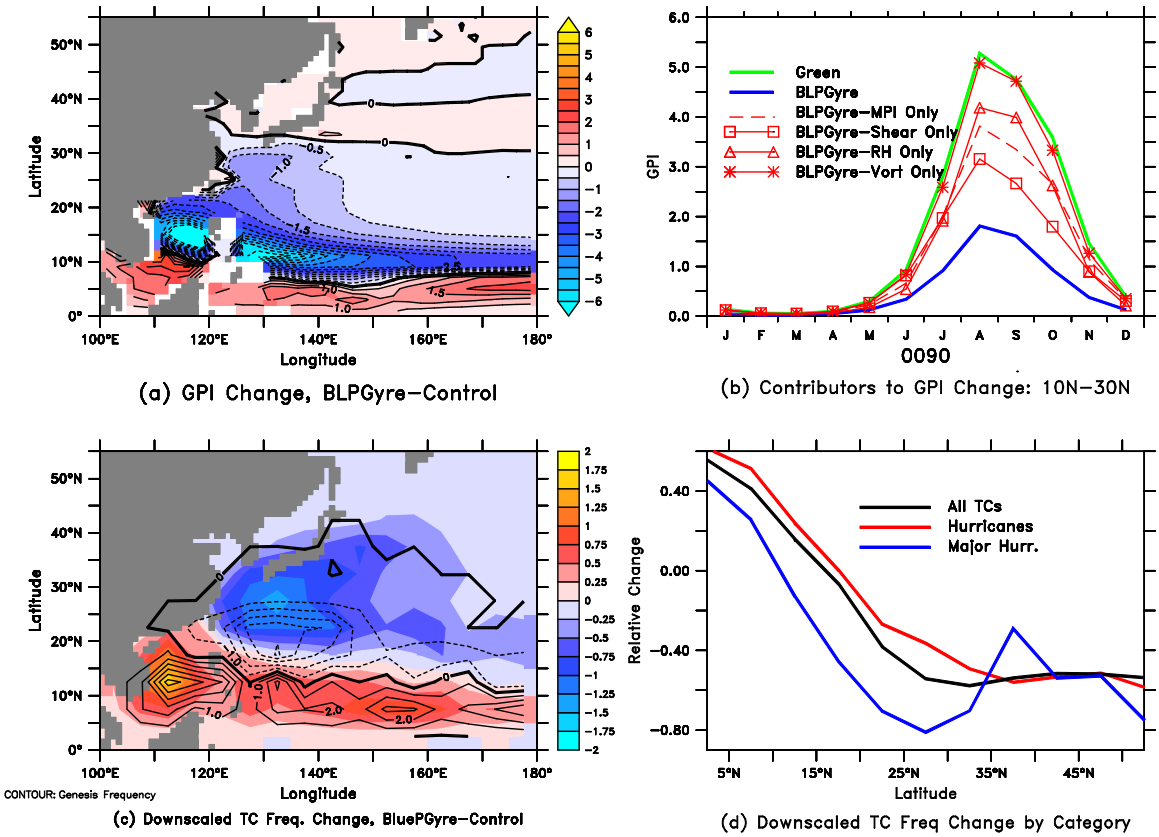

Figure 3: Changes in TC activity BLPGyre-Control. (a) Change in GPI. (b) Contributors to the change in GPI from 120W-180W, 10N-30N. (c) Difference in TC frequency (colors) and genesis frequency (contours) from statistical-dynamical downscale. (d) Relative change in TC frequency as a function of latitude for differing storm magnitudes from statistical-dynamical downscale. “Hurricanes” refer to storms with winds >33m/s. “Major hurricanes” have winds >49 m/s.

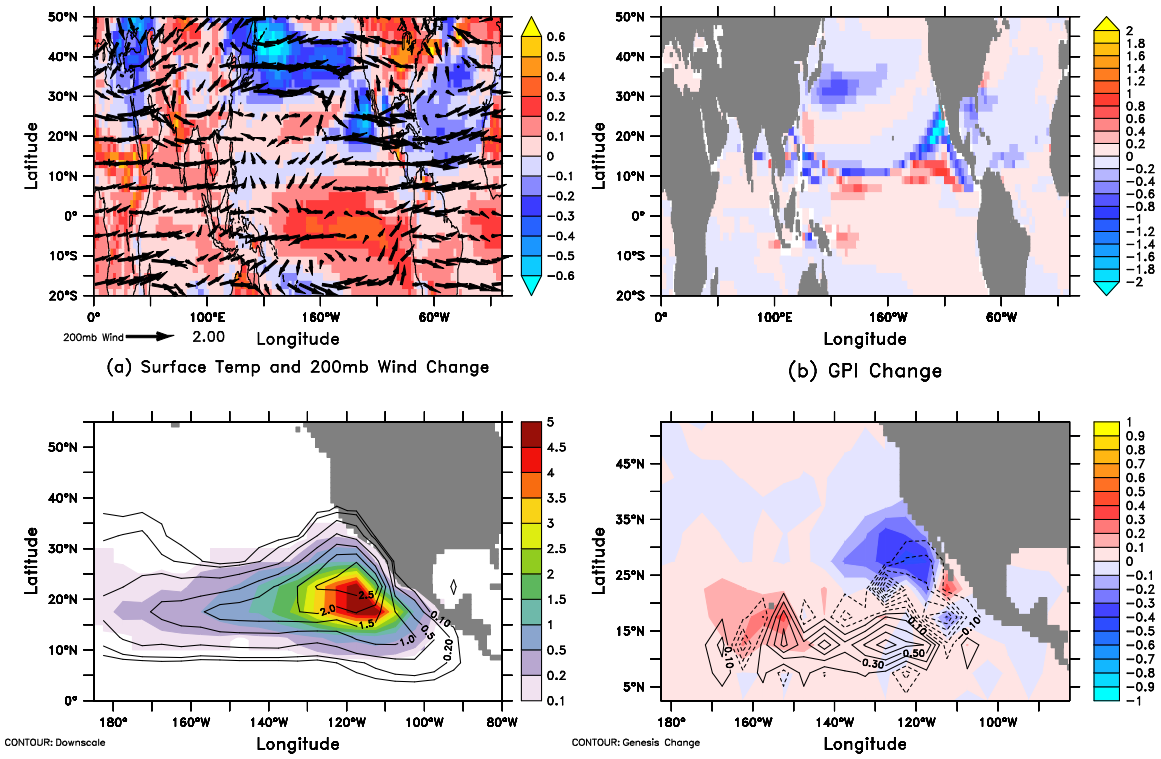

Figure 4: Impacts of changing solar penetration formulation from one penetrating band to three penetrating bands with a minimum mixed layer of 2m (corresponds to increasing penetration of sunlight). (a) Surface temperature and 200 mb wind change. (b) GPI change. (c) Comparison of observed TC frequency (days/yr, colors) and downscaled TC frequency for three band case (contours). (d) Change in frequency (colors) and genesis (TC/decade/5 degree bin) for three band case relative to one band case.